Available online at www.sciencedirect.com
SCIENCE DIRECT
Journal of the European Ceramic Society 26 (2006) 481–486
www.elsevier.com/locate/jeurceramsoc

The densification of zeolite/apatite composites using a pulse electric current sintering method: A long-term assurance material for the disposal of radioactive waste

Yujiro Watanabe [a,*], Toshiyuki Ikoma [b], Yasushi Suetsugu [b], Hirohisa Yamada [c], Kenji Tamura [c], Yu Komatsu [a], Junzo Tanaka [b], Yusuke Moriyoshi [d]

[a] *Faculty of Engineering, Kanazawa Institute of Technology, 7-1 Ohgigaoka, Nonoichi, Ishikawa, 921-8510, Japan*
[b] *Biomaterials Center, National Institute for Materials Science, 1-1 Namiki, Tsukuba, Ibaraki 305-0044, Japan*
[c] *Ecomaterials Center, National Institute for Materials Science, 1-1 Namiki, Tsukuba, Ibaraki 305-0044, Japan*
[d] *Faculty of Engineering, Hosei University, 3-7-2 Kajinocho, Koganei, Tokyo 184-8584, Japan*

Available online 22 August 2005

Abstract

Pulse electric current sintering (PECS) method was applied to the fabrication of zeolite, hydroxyapatite (HAp) and fluorapatite (FAp) sintered bodies that should be long-term assurance materials for the disposal of radioactive waste. The weight ratio of zeolite and apatite was ca. 3/7. Zeolite powder evenly covered with HAp thin layers prepared by a hydrothermal method and spherical FAp powder by spray dryer were employed for the PECS; the sample was sintered at 900 °C for 10 min at a rate of 50 °C/min under a uniaxial pressure of 50 MPa and then cooled to 600 °C at 5 °C/min in vacuum. The powder X-ray diffractions indicated that the structure of zeolite changed to the amorphous. The zeolite powder was well dispersed in FAp matrix as the results of element mapping analyses by energy dispersive X-ray spectrometer. The observations by a scanning transmission electron microscope indicated that amorphous zeolites were covered with needle-like HAp crystals of which layer completely coupled with sintered FAp grains. The HAp thin layers thus play an important role for improving the affinity between FAp matrix and the zeolite. The microhardness and three-point bending strength of the sintered bodies were also elucidated by a dynamic-ultra microhardness tester and a universal tester, respectively.

Keywords: Apatite; Composites; Nuclear applications; Sintering; Zeolite

1. Introduction

High-level radioactive elements, such as cesium, strontium and iodine, are discharged in the processes of nuclear power generation and nuclear reprocessing. These levels are controlled by legislation on discharge limits in many countries. It is, thus, important to develop long-term assurance materials for adsorbing, fixing and preserving radioactive elements over a long period of time.

More than 100 different species of synthetic zeolites have been identified.[1] Zeolites consist of a three-dimensional open-framework structure composed of AlO_4 and SiO_4 tetrahedra linked together by oxygen sharing with a three-dimensional open framework. The cations and water molecules diffuse through the channels and cavities as ion-exchange sites. Of the synthesized zeolite, Linde type-A zeolite ($(X_{12/n})(Si_{12}Al_{12}O_{48})\cdot 24H_2O$, X = cation, n = cation valence, LTA) with α- and β-cages has the highest cation exchange capacity (CEC).[2] Therefore, LTA is widely used as an adsorbent for harmful and radioactive elements.[3–7]

Hydroxyapatite ($Ca_{10}(PO_4)_6(OH)_2$, HAp) has a very low solubility of 5.4×10^{-119} (Ksp; $mol^{18}\,l^{-18}$) at a neutral pH solution, and shows high stability in an alkaline solution. Furthermore, the Ksp of fluorapatite ($Ca_{10}(PO_4)_6F_2$, FAp) is 8.1×10^{-121}, which is lower than that of HAp.[8] The HAp and/or FAp sintered bodies have been studied as one of long-term assurance matrices for preserving the radioactive

* Corresponding author. Tel.: +81 76 248 9504; fax: +81 76 294 6723.
E-mail address: Yujiro@neptune.kanazawa-it.ac.jp (Y. Watanabe).

0955-2219/$ – see front matter © 2005 Elsevier Ltd. All rights reserved.
doi:10.1016/j.jeurceramsoc.2005.07.032

elements.[9] Akao et al. described the dense HAp sintered bodies by using a conventional sintering method[10,11] and a post sintering method.[12] Pulse electric current sintering (PECS) method[13–15] can fabricate the dense HAp sintered bodies with approximately 100% of relative density at lower temperature and shorter duration compared to the conventional sintering method due to the rapid heating rate.

In our previous studies,[16,17] LTA with HAp thin layers was prepared by hydrothermal method in the cation exchange processes of Ca^{2+} to NH_4^+. This treatment did not destroy the cubic automorphism but changed its surface morphology by covering completely with nano-HAp scaly particles. We expect that the HAp thin layers play an important role for improving the affinity between FAp as matrix and zeolite in a sintering process.

In this study, the sintered bodies of LTA with HAp thin layers and FAp were fabricated by using the PECS method. The composites were characterized by XRD, SEM and STEM. The microstructure and mechanical properties of the sintered bodies were elucidated by using the dynamic-ultra-microhardness tester and universal tester.

2. Experimental procedures

2.1. Preparation of LTA with Ca^{2+} and HAp thin layers on its surface

LTA powder (<200 meshes) with Na^+ (Na-LTA) was purchased from Wako Pure Chemicals, Ltd., Japan. The complete cation exchange of Na^+ for Ca^{2+} was carried out by reacting 5.0 g of Na-LTA in 500 ml of 0.5 mol/l $CaCl_2$ solution for 1 h. This process was repeated three times. The resultant solid was isolated with a membrane filter of 0.45 μm in pore size, and washed with distilled water to remove excess cations. The LTA with Ca^{2+} (Ca-LTA) was obtained after dried at 100 °C for 24 h. The hydrothermal treatment was conducted as follows. One gram of Ca-LTA powder was immersed in 20 ml of 1.0 mol/l ammonium phosphate ($(NH_4)_3PO_4$) solution in a 100 ml Teflon cup fitted into a stainless-steal pressure vessel. The pH value of the solution was adjusted to 9 by adding an ammonium solution. The sample was heated at 120 °C for 8 h and quenched, washed three times with distilled water and dried at 100 °C for 24 h. The samples were characterized by X-ray diffractometer (XRD, Rigaku RINT2200, Japan) and scanning electron microscope (SEM, Jeol, JSM-5600LV, Japan).

2.2. Synthesis of spherical FAp powder

H_3PO_4 solution (6.0 mol/l) and 2.0 mol/l of HF solution was mixed and aged for 1 day in N_2 gas. The mixed solution was dropped slowly into 10.0 mol/l $Ca(OH)_2$ suspension with vigorous stirring at room temperature. The molar ratio of Ca^{2+}, PO_4^{3-} and F^- was adjusted to 10, 6 and 2. The resultant mixture was then aged for 1 day, and the final pH was about 7.0. Spherical FAp powder was fabricated by a spray dryer (DL-41, YAMATO Sci. Co., Ltd, Japan). The suspension was atomized under a pressure of 1.5 MPa at a flow rate of 500 ml/h, and inlet and outlet temperatures of a nozzle were adjusted to 180 and 80 °C, respectively. The spray-dried FAp powder was calcined at 800 °C for 3 h to increase the crystallinity. The resultant sample was characterized by XRD and SEM.

2.3. Fabrication of LTA with HAp thin layers/FAp sintered bodies

The LTA with HAp thin layers and the spherical FAp powder were mixed at a weight ratio of 3/7. The obtained powder was sintered by using a pulse electric current sintering method (PECS, Sumitomo Coal Mining, SPS-1030, Japan). The sample was pressed uniaxially at 50 MPa in the vacuum of 0.6×10^{-2} Pa throughout the sintering process. The temperature was increased to 900 °C at a rate of 50 °C/min. After keeping at 900 °C for 10 min, the sample was slowly cooled to 600 °C at a rate of 5 °C/min. The sample was cooled further to room temperature after stopping the electric current and releasing the pressure. The sintered bodies with 20 mm in diameter and 4 mm in thickness were characterized by using XRD and SEM after polishing. The element mapping analyses were carried out with an energy dispersive X-ray spectrometer (EDX, Jeol, JRD2200, Japan) equipped with SEM.

The boundary structure in the sintered body with three different phases, i.e. LTA, HAp and FAp, was observed by a scanning transmission electron microscope (STEM, Hitachi, HF2210, Japan). The element in the boundary structure was analyzed by an energy dispersive X-ray spectrometer (EDX, Genesis4000, USA). The specimen with 100 nm in thickness was prepared by a focused ion beam method (FIB, Noran Vantage: FB-2100, USA) and a pick-up method.

The microhardness of the sintered bodies was measured with a dynamic-ultra- microhardness tester (Shimadzu, DUH-W201, Japan). The three-point bending strength and Young's moduli were measured using a universal tester (Shimadzu, AGS-H, Japan) with a crosshead speed of 1 mm/min. The size of the sample was 18 mm × 3 mm × 1 mm and the number of samples for bending strength and Young's moduli measurement was five. The measurements were conducted three times to give the average values.

3. Results and discussion

3.1. Characterization of Ca-LTAs and spherical FAp

The Ca-LTA powder with the complete exchange of Na^+ for Ca^{2+} in LTA was obtained, judged from the change of diffraction intensities and the appearance of a new diffraction

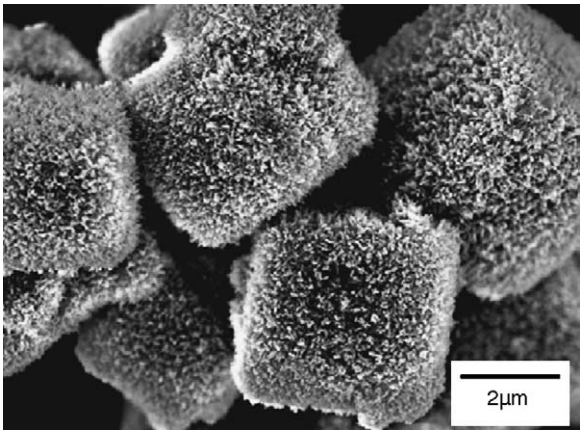

Fig. 1. The SEM image of LTA with HAp thin layers prepared by the hydrothermal treatment at 120 °C.

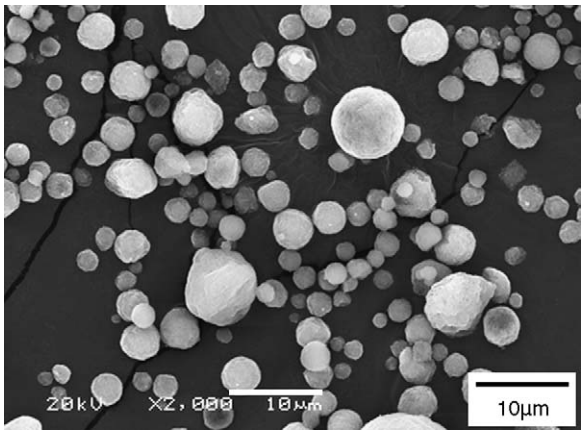

Fig. 2. The SEM image of spherical FAp particles prepared by the spray dryer.

at 25.1° in 2θ by XRD. After the hydrothermal treatment of Ca-LTA, the broad diffractions at about 26° and 32° in 2θ were found, which were corresponded closely to the diffractions of HAp.[16]

Fig. 1 shows SEM image of the resultant LTA after the hydrothermal treatment. The hydrothermal treatment did not destroy the cubic automorphism but changed its surface morphology by complete covering with scaly particles. The scaly particles were aggregates of needle-like HAp crystals and formed HAp thin layers. We previously studied the morphological details of HAp nanocrystals on the zeolite surface.[16,17]

Fig. 2 shows the SEM image of FAp powder obtained by the spray dryer and calcined at 800 °C for 3 h. The FAp powder was spherical in shape, and the particle size was about 1–10 μm. The XRD pattern showed only diffractions of FAp. Calcination at 800 °C was necessary to increase the crystallinity of FAp. This powder was employed for the starting material of the PECS method.

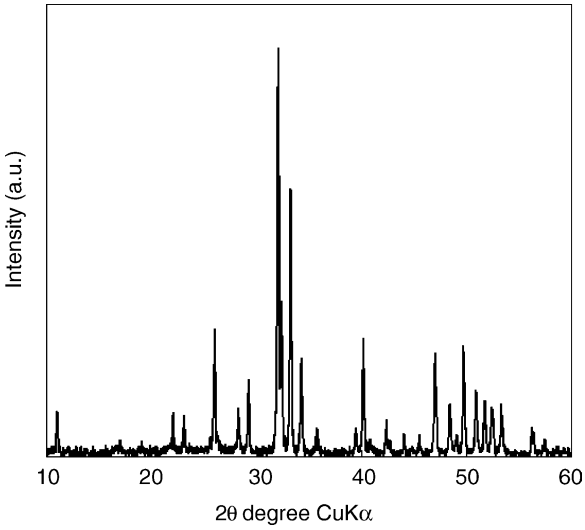

Fig. 3. The XRD patterns of the sintered body obtained at 900 °C.

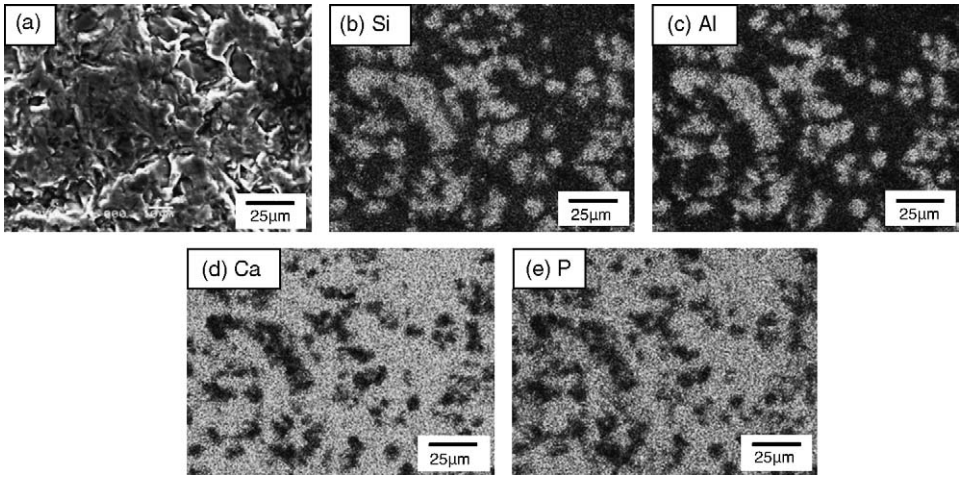

Fig. 4. The SEM image (a) and element mappings (Si (b), Al (c), Ca (d) and P (e)) of the sintered body obtained at 900 °C by PECS.

3.2. Characterization of LTA with HAp coating layers/FAp sintered bodies

Fig. 3 shows the XRD pattern of the sintered body of LTA with HAp thin layers and FAp. The XRD pattern identified only FAp phase, which is explained by a phase change of LTA to amorphous by the PECS method. From the results of XRD and Fourier-transform infrared spectroscopy, we confirmed that the Ca-LTA after hydrothermal treatments changed to LTA with NH_4^+ (NH_4-LTA).[16] Chandrasekhar and Pramada[18] reported that the NH_4-LTA calcined at 850 °C had an amorphous structure whereas the structure remained intact at 750 °C, and mullite started crystallizing at 950 °C. In the present study, the temperature increased to 900 °C at a heating rate of 50 °C/min and held for 10 min. The heating rate and holding time were much less than the rate of 3 °C/min and 3 h in a furnace described by Chandrasekhar and Pramada[18] We conclude from these results that the LTA in the sintered bodies changes to an amorphous phase under the sintering condition. Therefore, the diffraction pattern of LTA in the sintered bodies was not detected by XRD.

Fig. 4a shows the SEM image of the surface of sintered bodies, and Fig. 4b–e show EDX mapping results of the Si, Al, P and Ca elements. The sintered body was well densified, and the grains were very small (<1 μm). There is no significant difference in the crystal morphology of FAp and LTA. Thus, the elemental mapping analyses of Si, Al, Ca and P on the surface of the sintered body were useful to distinguish the components. The main components of LTA were Si and Al, which located in the same positions in their distribution. The particle size of the amorphous parts was about 5 μm that corresponds with that of LTA with HAp thin layers as shown in Fig. 1. The Ca and P were distributed in the same positions, which were the main component of FAp and HAp. These results indicated that the amorphous phase was completely covered by FAp and HAp. The HAp thin layers on LTA surface play an important role for preventing the binding among zeolite powders.

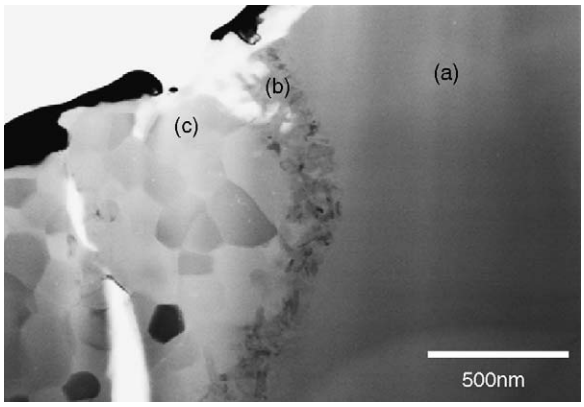

Fig. 5. The STEM image of the sintered body obtained at 900 °C by PECS. (a) LTA (the amorphous phase) (a), HAp (b) and FAp (c).

Fig. 5 shows the STEM image of the sintered body of LTA with HAp thin layers and FAp. The HAp thin layers were clearly observed at the interface between amorphous LTA and FAp. The shape and size of HAp thin layers were needle-like crystals about 150 nm in length. The size was almost matched to that of HAp grown on the surface of LTA as shown in Fig. 1. The FAp crystals in the sintered bodies were well sintered, and the grain size was small (<300 nm). Micropores were not observed among the three different phases. It indicates that

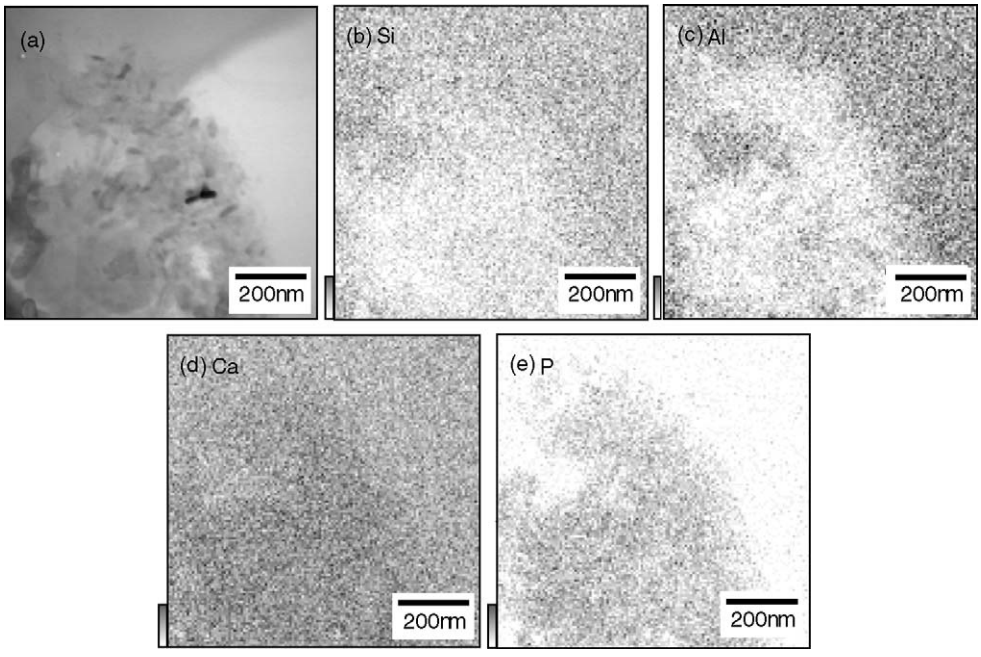

Fig. 6. The STEM image (a) and element mappings (Si (b), Al (c), Ca (d) and P (e)) of the sintered body obtained at 900 °C by PECS.

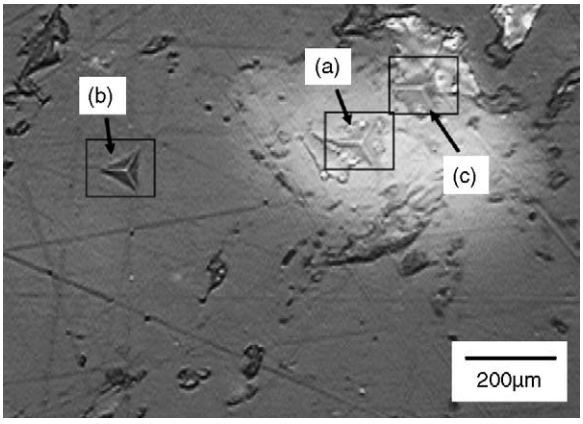

Fig. 7. The optical microscope images of indentations of pyramidal indenters (115°) on (a) LTA, (b) FAp and (c) the interface between LTA and FAp in the sintered body by a dynamic-ultra-microhardness tester.

Table 1
The load, depth and dynamic hardness calculated from indentations of FAp and HAp and the interface

	P_G (gf)	D (μm)	DH
FAp	20	1.11	612
LTA	20	1.31	448
Interface	20	1.30	441

P_G: load, D: depth DH: dynamic hardness.

the three different phases are completely sintered, and the HAp layers play an important role for improving the affinity between FAp and amorphous LTA. When the mixed powder of LTA and FAp without HAp thin layers was sintered under the same condition, the sintered bodies obtained were with cracks and/or destroyed in ejecting. Fig. 6 shows the mapping images obtained by EDX equipped with STEM. Si and Al were distributed in the position of amorphous LTA, and P was distributed in the positions of HAp and FAp. Ca was distributed mainly in the positions of FAp and HAp, but the distribution was less dominant in the position of LTA. These results indicate that Ca ions barely remain in the LTA.

3.3. Mechanical properties of LTA with HAp coating layers/FAp composites

Fig. 7 shows optical microscope images of indentations of pyramidal indenters (115°) on LTA (a), FAp (b) and the interface between LTA and FAp (c) on the sintered bodies. Table 1 shows the load (P_G, gf), depth (D, μm) and dynamic hardness (DH) calculated from indentations. The DH in a pyramidal indenter is defined by the following formula: $DH = 37.838\,P_G/D^2$. The DH of FAp was 612, which was larger than those of amorphous LTA (a) (DH = 448) and the interface (c) (DH = 441). We considered that the LTA changed to an amorphous phase is weak in strength, and the interface between the phase and FAp is similarly weak in strength.

The average three-point bending strength was 54 MPa, and the Young's modulus was 30 GPa which was considerably lower than that of FAp sintered bodies (three-point bending strength: 162 MPa, Young's modulus: 85 GPa. These results also indicate that the interface between an amorphous LTA and FAp is similarly weak in strength.

4. Conclusion

The fabrication of sintered body of LTA with HAp thin layers and FAp was succeeded by using the PECS method at 900 °C. The LTA phase changed to an amorphous phase under this condition. The amorphous LTA in the sintered bodies was completely surrounded by HAp and FAp. The microstructural observations indicated that the three different phases (the amorphous LTA, HAp and FAp) were completely sintered. The HAp thin layers played an important role for improving the affinity between FAp and LTA in sintering. The microhardness of the amorphous LTA and the interface of amorphous LTA and FAp were lower than that of FAp, and three-point bending strength was also lower than that of FAp.

Acknowledgements

The authors are indebted to Dr. H. Nishimura, National Institute for Materials Science for his kind help in PECS and discussion. A part of this study was financially supported by the Budget for Nuclear Research of the Ministry of Education, Culture, Sports, Science and Technology, based on the screening and counseling by the Atomic Energy Commission.

References

1. Meier, W. M., Olson, D. H. and Baerlocher, C., Atlas of zeolite structure types. *Zeolites*, 1996, **17**, 1.
2. Breck, D. W., Structure of zeolites. In *Zeolite Molecular Sieves*, ed. D. W. Breck. Wiley, New York, 1974, pp. 29–185.
3. Watanabe, Y., Yamada, H., Kokusen, H., Tanaka, J., Moriyoshi, Y. and Komatsu, Y., Ion exchange behavior of natural zeolites in distilled water, hydrochloric acid, and ammonium chloride solution. *Sep. Sci. Technol.*, 2003, **38**, 1519–1532.
4. Watanabe, Y., Yamada, H., Tanaka, J., Komatsu, Y. and Moriyoshi, Y., The adsorption of ammonium ions on synthetic zeolites: the effect of their open-window sizes, pore structures, and cation exchange capacities. *Sep. Sci. Technol.*, 2004, **39**, 2091–2104.
5. Watanabe, Y., Yamada, H., Kokusen, H., Tanaka, J., Moriyoshi, Y. and Komatsu, Y., Effect of cage-size on ammonium adsorption by synthetic zeolites. In *Proceedings of the 18th International Japan-Korea Seminar on Ceramics*, 2001, pp. 543–547.
6. Mimura, H. and Akiba, K., Adsorption behavior of cesium and strontium on synthetic zeolite-P. *J. Nucl. Sci. Technol.*, 1993, **30**, 436–443.
7. Song, K. C., Lee, H. K., Moon, H. and Lee, K. J., Simultaneous removal of the radiotoxic nuclides Cs-137 and I-129 from aqueous solution. *Sep. Purif. Technol.*, 1997, **12**, 215–227.
8. Moreno, E. C., Kresak, M. and Zaharadnik, R. T., Fluoridated hydroxyapatite solubility and caries formation. *Nature*, 1974, **24**, 64–65.
9. Yanagisawa, I., Izumi, J., Tomonaga, N., Kitao, H., Neyama, A. and Katurai, K., I-129 fixation by silica coated zeolite distributed in extremely low solubility non-organic matrix multi-layered distributed

waste-form for I-129. *J. Nucl. Fuel Cycle Environ.*, 1999, **6**, 67–69 (in Japanese).
10. Akao, M., Aoki, H. and Kato, K., Mechanical-properties of sintered hydroxyapatite for prosthetic applications. *J. Mater. Sci.*, 1981, **16**, 809–812.
11. Ikoma, T., Yamazaki, A., Nakamura, S. and Akao, M., Preparation and dielectric property of sintered monoclinic hydroxyapatite. *J. Mater. Sci. Lett.*, 1999, **18**, 1225–1228.
12. Takikawa, K. and Akao, M., Fabrication of transparent hydroxyapatite and application to bone marrow derived cell/hydroxyapatite interaction observation in-vivo. *J. Mater. Sci. Mater. Med.*, 1996, **7**, 439–445.
13. Gu, Y. W., Loh, N. H., Khor, K. A., Tor, S. B. and Cheang, P., Bone-like apatite layer formation on hydroxyapatite prepared by spark plasma sintering (SPS). *Biomaterials*, 2002, **23**, 37–43.
14. Nakahira, A., Tamai, M., Aritani, H., Nakamura, S. and Yamashita, K., Biocompatibility of dense hydroxyapatite prepared using an SPS process. *J. Biomed. Mater. Res.*, 2002, **62**, 550–557.
15. Watanabe, Y., Ikoma, T., Monkawa, A., Suetsugu, Y., Yamada, H., Tanaka, J. *et al.*, Fabrication of transparent hydroxyapatite sintered body with high crystal orientation by pulse electric current sintering. *J. Am. Ceram. Soc.*, 2005, **88**, 243–245.
16. Watanabe, Y., Moriyoshi, Y., Hashimoto, T., Suetsugu, Y., Ikoma, T., Kasama, T. *et al.*, Hydrothermal preparation of type-A zeolite with hydroxyapatite surface layers. *J. Am. Ceram. Soc.*, 2004, **87**, 1395–1397.
17. Watanabe, Y., Moriyoshi, Y., Hashimoto, T., Kasama, T., Suetsugu, Y., Ikoma, T. *et al.*, Characterization of type-A zeolite with hydroxyapatite surface layer prepared by hydrothermal treatment. In *Proceedings of the 20th International Japan–Korea Seminar on Ceramics*, 2003, pp. 213–216.
18. Chandrasekhar, S. and Pramada, P. N., Sintering behaviour of ammonium exchanged low silica zeolites synthesised by two different routes. *Ceram. Int.*, 2001, **27**, 351–361.